



Impedimetric immunosensor for dengue diagnosis using graphite screen-printed electrodes coated with poly(4-aminophenylacetic acid)

Thiago Coimbra Pimenta¹ · Cátia da Cruz Santos¹ · Ronaldo Luís Thomasini² · Lucas Franco Ferreira¹ 

Published online: 4 September 2018
© Springer Science+Business Media, LLC, part of Springer Nature 2018

Abstract

Dengue is an infectious viral disease transmitted by the *Aedes aegypti* mosquito, the control of which is complex. In addition, the clinical diagnosis is difficult to perform since it resembles other febrile infections; thus, the development of more effective methods to detect dengue virus (DV) has drawn increasing attention. The present study aimed to develop an impedimetric immunosensor for dengue diagnosis using a screen-printed electrode (SPE) functionalized with polymer films derived from 4-aminophenylacetic acid (4-APA). Data obtained from scanning electron microscopy (SEM) showed the deposition of a uniformly distributed material over the electrode surface. The immunosensor was based on the specific interaction between dengue antigen, NS1 protein, and anti-NS1 antibodies, IgG and IgM. In a characterization study using cyclic voltammetry (CV), the polymer film showed two oxidation peaks at +0.17 and + 0.35 V in 0.50 M sulfuric acid solution, indicating its adsorption and electroactivity at the SPE surface. Electrochemical impedance spectroscopy (EIS) measurements showed a higher charge transfer resistance (R_{ct}) to the polymer film-modified SPE as compared with the bare SPE, corroborating a previous study. The best rNS1 concentration for immobilization was 1.00 ng/mL, and the immunoreaction time between the antigen (Ag) and the antibody (Ab) was 20 min. Dilutions of positive and negative clinical serum samples were evaluated by EIE, from which it was possible to elucidate, for the positive serum, that the more diluted the serum the greater the R_{ct} . Negative serum also showed an analytical signal, probably due to the presence of non-specific antibodies; however, the generated signal presented values closer to the rNS1 signal, indicating good selectivity of the proposed platform. The experiments were repeated using bare SPE to verify the importance of the polymer film in biosensor construction. No significant difference was observed between these results.

Keywords Immunosensor · 4-aminophenylacetic acid · Electropolymerization · Polymer films · NS1 · Dengue

1 Introduction

Dengue is an infectious viral disease transmitted by mosquitoes from the *Aedes* genus, which is mostly found in tropical and subtropical areas. According to the World Health Organization (WHO), approximately 3.9 billion people live in the area where dengue is endemic, and it is estimated that there are 390 million new dengue infections per year, of which

96 million manifest clinically. In 2015, 2.35 million cases of dengue were reported in the Americas alone, of which 10,200 cases were diagnosed as severe dengue, causing 1181 deaths (World Health Organization 2017).

The early diagnosis of the disease is very important to avoid the spread of the virus and to initiate appropriate medical care, which leads to a significant decrease in mortality (World Health Organization 2012). In this context, there is an urgent need for rapid diagnosis and prophylactic vaccines aiming at increasing the quality of life of the people who live in high-risk areas. The major methods used for the diagnosis of dengue fever (DF) are reverse-transcription polymerase chain reaction (RT-PCR) and monoclonal antibody capture-enzyme linked immunosorbent assay (MAC-ELISA) (Mackay 2004); however, PCR-based methods are fairly expensive, take more time than serological tests, and are not commonly accessible in major developing countries (Sinawang et al. n.d.). On the other hand, serological evaluation has several limitations, including a prolonged time to seroconversion (3–7 days), serological persistence of IgM

✉ Lucas Franco Ferreira
lucas.franco@ict.ufvjm.edu.br

¹ Laboratório de Eletroquímica e Nanotecnologia Aplicada, Instituto de Ciência e Tecnologia, Universidade Federal dos Vales do Jequitinhonha e Mucuri, Rodovia MGT 367, Km 583, 5000, Alto da Jacuba, Diamantina-MG 39100-000, Brazil

² Faculdade de Medicina, Universidade Federal dos Vales do Jequitinhonha e Mucuri, Rodovia MGT 367, Km 583, 5000, Alto da Jacuba, Diamantina-MG 39100-000, Brazil

antibodies following disease resolution, and cross-reactivity with other flaviviruses (Hunsperger et al. 2009; Tang and Ooi 2012).

Recently, the detection of dengue virus (DV) nonstructural protein 1 (NS1) has emerged as a potential alternative to both serological and molecular-based techniques for the diagnosis of active dengue infection (World Health Organization 2012; Simmons et al. 2012; Wang and Sekaran 2010). NS1 is a highly conserved glycoprotein in flaviviruses, which possesses both group-specific and type-specific determinants and is essential for viral viability. It can be detected within 24 h and up to nine days following the onset of symptoms (Falconar and Young 1991; Henchal et al. 1987). Kinetically, NS1 antigenemia overlaps with the dengue viremic phase and is present prior to IgM seroconversion, making the NS1 antigen an ideal biomarker for the identification of acute dengue infection (Flamand et al. 1999; Kassim et al. 2011).

Electrochemical biosensors have drawn attention due to the possibility of miniaturization of the system, high sensitivity, and low-cost; and are also promising for a wide range of biomedical and environmental applications (Wang 2002, 2005). Screen-printed electrodes (SPE) have become attractive in the development of such devices, since they are versatile, easier to mass produce, and suitable for in loco application (Somerset et al. 2010; Silva et al. 2014). An immunosensor can be obtained by exploiting the unique phenomenon of antigen–antibody interaction, and is appropriate for the development of a tool for dengue diagnosis, since SPE can combine good electrochemical properties with portability, which could be of extreme interest to countries in which clinical care is poor. Furthermore, combining polymer properties with those of biological components makes it possible to develop a bioelectronic sensor system.

Conductive polymers under thin films form deposits on the electrode surface, representing promising materials for the application of sensors (McQuade et al. 2000) and biosensors (Adhikari and Majumdar 2004) where a recent tendency in this area is the use of functionalized conductive polymers (Júnior et al. 2004), which can ensure higher stability/durability of the biomolecule immobilization process, decreasing the lexiviation effect and loss of biosensor response. The aim of the present study was to develop an impedimetric immunosensor using an SPE modified with a polymer film from 4-aminophenylacetic acid (4-APA) for application in dengue diagnosis based on antibody detection. To the best of our knowledge, this is the first study regarding 4-APA electropolymerization and its use in immunosensor development for dengue diagnosis.

2 Experimental

2.1 Apparatus and reagents

All electrochemical measurements were carried out using a Pontenciostat/Galvanostat from Autolab®, model PGSTAT

128 N, and carbon screen-printed electrodes from DropSens®. The data were acquired using version 1.10 of the NOVA software. All chemicals used were of analytical grade. The solutions were prepared with ultrapure water (18.2 MΩ.cm) from a Master System MS 2000 Gehaka (<https://www.gehaka.com.br>).

Sulfuric acid, potassium chloride, sodium chloride, potassium ferricyanide/ferrocyanide, 4-aminophenyl acetic acid (4-APA), HEPES, and EDTA were purchased from Sigma-Aldrich (<http://www.sigmaaldrich.com.br>). HBS-EP buffer solution (pH 7.4) was prepared by mixing 10 mM HEPES pH 7.4, 3.0 mM EDTA pH 8.0, and 15 mM NaCl.

Recombinant dengue non-structural 1 protein (rNS1) was produced by isopropyl β-D-1thiogalactopyranoside (IPTG) induction in *Escherichia coli* BL21 rosetta transformed with the Pet-28a (+) plasmid containing the NS1 sequence (Dengue 2, Maynnar strain MM-2, Genbank Accession Number: U51929), and purified by immobilized nickel column affinity chromatography – IMAC (protein contained a poly-histidine tag).

2.2 Electropolymerization of 4-APA

Prior to the electropolymerization step, the SPEs were analyzed/conditioned by cyclic voltammetry (CV) via the addition of 60 μL 0.50 M sulfuric acid solution to the electrode surface. A volume of 60 μL aqueous 5.0 mM potassium ferrocyanide/ferricyanide solution containing 0.10 M KCl was also used. In these steps, three consecutive cycles were performed in the presence of 0.50 M sulfuric acid at a potential range of −0.20 to +0.90 V, and one cycle in the presence of $K_4Fe(CN)_6 / K_3Fe(CN)_6$, at a potential range of −0.55 to +0.80 V.

Electropolymerization of 4-APA over the SPE was performed by CV. The cyclic voltammograms were recorded at a potential range of −0.20 to +0.90 V, with 10 consecutive cycles in 2.50 mM aqueous 4-APA solution containing 0.50 M sulfuric acid.

2.3 Morphological study

Non-modified SPE and poly(4-AFA)/SPE were characterized by Scanning Electron Microscopy (SEM) using a model TM-3000 tabletop microscope from Hitachi. Images were obtained at 30 kV using the backscattered electrons detected in composed mode.

2.4 Electrochemical properties of 4-APA

The electrochemical properties of the bare SPE and the SPE modified with poly(4-APA) – poly(4-APA)/SPE – were investigated by CV using a potassium ferricyanide/ferrocyanide redox probe at 5.00 mM containing 0.10 M

KCl, sweeping at a potential range of -0.55 to $+0.80$ V. CV was also performed on the supporting electrolyte solution (0.10 M KCl) at the same potential region of the redox pair to verify the electroactive contribution of the film formed during the redox process.

2.5 Electrochemical impedance spectroscopy (EIS) measurements

The electrochemical impedance spectroscopy measurements of SPE, poly(4-APA)/SPE, and poly(4-APA)/SPE immobilized with the rNS1 protein (rNS1/poly(4-APA)/SPE), and subsequent interaction of the immunosensor with the positive (Ab^+ /rNS1/poly(4-APA)/SPE) and negative (Ab^- /rNS1/poly(4-APA)/SPE) sera, were obtained in 5.0 mM $K_4[Fe(CN)_6]/K_3[Fe(CN)_6]$ aqueous solution containing 0.10 M KCl. The analytical solution was deoxygenated with ultra-pure gaseous nitrogen for approximately 10 min prior to measurement. The investigated frequency range was 10^5 to 10^{-2} Hz, and the sinusoidal excitation amplitude was 10 mV, with the application of an open circuit potential (OCP).

2.6 rNS1 immobilization and anti-NS1 antibody detection

rNS1 solutions at concentrations of 6, 3, 1, and 0.1 mg/mL, 10, 1, and 0.1 μ g/mL, and 1 ng/mL were prepared in HBS-EP buffer solution pH 7.40. Subsequently, eight SPEs previously modified with poly(4-APA) were separated for the immobilization of rNS1 at different concentrations, and 30 μ L of each solution was added to the working electrode surface. The SPEs were then incubated at 37 $^{\circ}$ C for 20 min, following which, they were washed with HBS-EP buffer solution pH 7.40, and dried under nitrogen gas for EIS recording.

For reaction with positive and negative clinical serum samples, dilutions were made in HBS-EP buffer solution pH 7.40 at ratios of 1:20, 1:40, 1:80, 1:160, 1:320, 1:640, and 1:1280. A volume of 30 μ L each solution was added onto the surface of electrodes previously modified with rNS1 (rNS1/poly(4-APA)/SPE), and incubated at 37 $^{\circ}$ C for 20 min. After this period, the electrodes were washed with HBS-EP buffer solution pH 7.40 and dried under nitrogen gas for EIS recording.

2.7 Immunoreaction time elucidation

For antigen–antibody (Ag/Ab) reaction time elucidation, 30 μ L positive (1:160 dilution) rNS1/poly(4-APA)/SPE ([rNS1] = 1 ng/mL) was added and incubated at 37 $^{\circ}$ C for 5, 10, 20, 40, and 80 min. The electrodes were subsequently

washed with HBS-EP buffer solution pH 7.40 and dried under nitrogen gas.

3 Results and discussion

The cyclic voltammogram related to the electropolymerization of 4-APA is shown in Fig. 1. During the first potential cycle, a peak corresponding to the oxidation of 4-APA at $+0.70$ V can be observed, indicating the formation of cation radicals, which are necessary to initiate the polymerization process. Two further peaks, one at $+0.18$ V and the other at -0.034 V, can also be observed, which are related to the reduction of the polymer film formed on the electrode surface.

Following the second potential cycle, it is possible to notice two oxidation waves that appear at the potentials of $+0.010$ and $+0.30$ V (inset of Fig. 1), corresponding to the oxidation of the film formed on the electrode.

Following successive cycles, a decrease in the anodic peak current at $+0.70$ V can be observed in addition to a small displacement of the oxidation potential to more positive ranges; and these events may be related to monomer consumption at the electrode surface for subsequent formation of the polymer film, which leads to a partial blockage of the electrode surface.

3.1 Morphological analysis

SEM images of the non-modified SPE and the poly(4-APA)/SPE were obtained as can be seen in Fig. 2. Comparing these two images, it can be noticed that the 4-APA electropolymerization process leads to a deposition of a material evenly distributed on the electrode surface. This result confirms the data presented by the

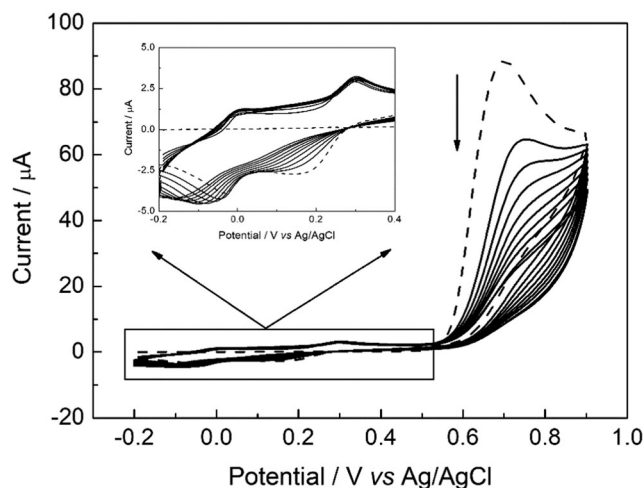
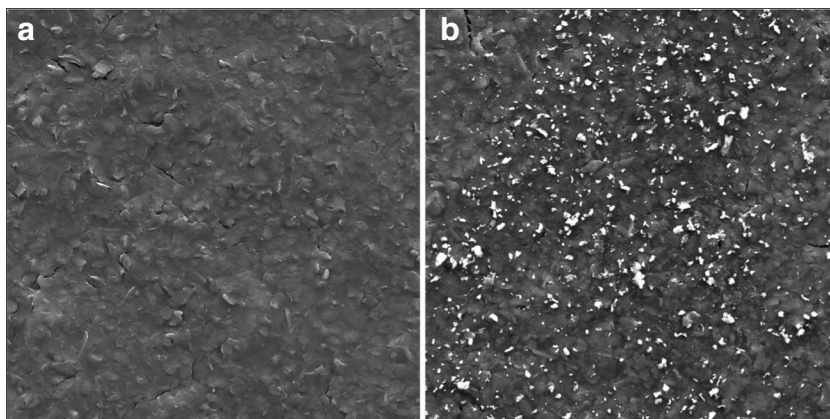


Fig. 1 Consecutive cyclic voltammograms of 4-APA (10 cycles) in 0.50 M H_2SO_4 solution at -0.20 to $+0.90$ V potential range. $v = 50$ mV/s. [4-APA] = 2.50 mM. (—) 1st potential cycle

Fig. 2 SEM images obtained for (A) SPE and (B) poly(4-APA)/SPE. Magnification of $\times 500$



CV and EIS studies, as discussed in items 3.2 and 3.3, respectively.

3.2 Electrochemical behavior and charge transfer properties of poly(4-APA)/SPE

The electrochemical behavior of the modified electrode was verified by CV in 0.50 M sulfuric acid, as shown in Fig. 3a. It can be noticed that there was a change in the electrochemical response of poly(4-APA)/SPE as compared with bare SPE, observing an electroactivity at +0.17 and +0.35 V. This result confirms the formation of an electroactive deposit on the electrode surface.

Figure 3b, c show the CVs of the bare SPE and poly(4-APA)/SPE obtained in 5.00 mM $K_3Fe(CN)_6/K_4Fe(CN)_6$ solution containing 0.10 M KCl to verify the electroactivity of the material adsorbed on the electrode surface against the redox probe, as well as to analyze its behavior in electrolyte support solution.

Figure 3b shows the oxidation and reduction peaks at +0.225 V and +0.034 V, respectively, for the bare SPE and at +0.371 V and -0.107 V, respectively, for the poly(4-APA)/SPE. It can be noticed that the anodic peak current (I_{pa}) and the cathodic peak current (I_{pc}) decreased, and the anodic potential (E_a) and cathodic potential (E_c) for the poly(4-APA)/SPE shifted as compared with the bare SPE. These results show that the modification of the SPE surface and the deposited polymer film hinder the electronic transfer process at the electrode/solution interface.

To verify that the poly(4-APA) film contributes to the effect observed in Fig. 3b, CV was performed in 0.10 M KCl at the same potential range of the redox pair (Fig. 3c). It can be observed that the cyclic voltammogram related to the poly(4-APA)/SPE showed a small oxidation peak at +0.132 V, and that for the SPE showed no electrochemical activity. Thus, it can be concluded that the polymer film electroactivity does not significantly contribute to the effect observed in Fig. 3b.

3.3 Electrochemical impedance spectroscopy analysis

The poly(4-APA)/SPE was assessed by EIS, and the data obtained were compared with that of the bare SPE. Figure 4 shows the Nyquist diagrams for both electrodes studied. The analysis shows two very distinct regions: a semicircle-shaped region at high frequencies, which is related to the charge transfer resistance, and another region at low frequencies, in which a line appears, relating to mass transfer by diffusion processes.

The semicircle formed in Fig. 4 by the poly(4-APA)/SPE had a larger diameter, and consequently, a greater charge transfer resistance as compared with the bare SPE. This suggests that the polymer film adsorbed on the electrode surface hinders the electronic transfer process of the redox pair that occurs at the electrode/solution interface.

The EIS data were obtained by applying a Randles circuit ($R_s(Q_{dl}[R_{ct}W])$) to the studied system, where R_s is the ohmic resistance of the solution; R_{ct} is the charge transfer resistance that occurs at the electrode/solution interface; Q_{dl} is the constant phase element that describes the pseudocapacitance of the double electric layer; and W is the Warburg impedance, which describes the electron diffusion-controlled processes.

Table 1 shows the values for each element of the circuit. It can be noticed that the R_s value for the bare SPE and poly(4-APA)/SPE barely changed, which is to be expected, since the analysis solution was the same in all measurements, indicating that the polymer film formed on the surface of the electrode does not influence the strength of the solution.

It can also be observed that the R_{ct} value for the bare SPE presented a low impedimetric response ($R_{ct} = 92.5 \Omega$), and following the electropolymerization step, there was an increase in the system resistivity of approximately 31 times ($R_{ct} = 2876 \Omega$) due to partial blockade of charge transfer at the double electric layer, which is corroborated by the graph in Fig. 3b, indicating the formation of poly(4-APA) on the electrode surface.

In addition, it can be observed that the system capacitance decreased for the modified electrode, which suggests that the electroactive area decreased, likely due to the adsorption of

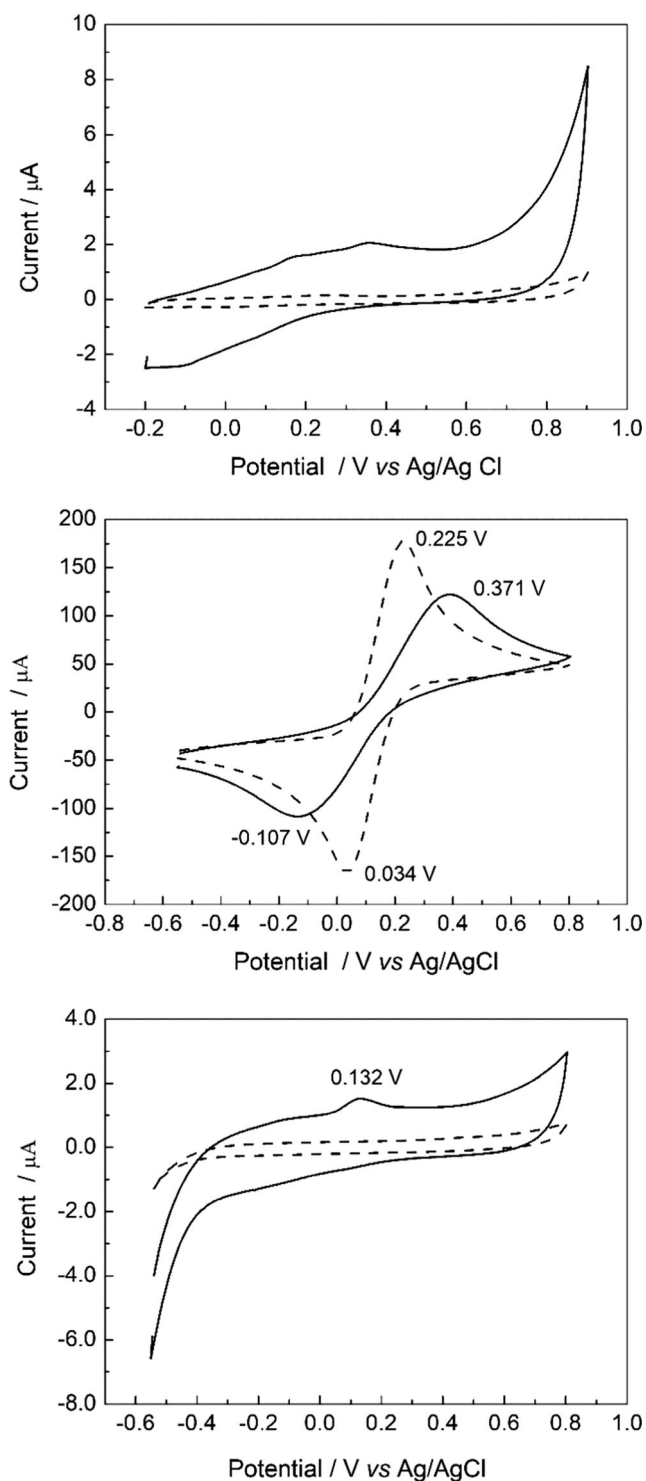


Fig. 3 Cyclic voltammograms for (—) SPE and (---) poly(4-APA)/SPE in: (A) 5.0 M H₂SO₄ solution; (B) 5.0 mM K₃Fe(CN)₆/K₄Fe(CN)₆ solution containing 0.10 M KCl; and (C) 0.10 M KCl solution. $\nu = 100$ mV/s

the polymer film on the electrode surface. This reduced transducer roughness and porosity, approaching a perfect capacitor, as observed by the increase in n_{dl} values for both the bare SPE and poly(4-APA)/SPE.

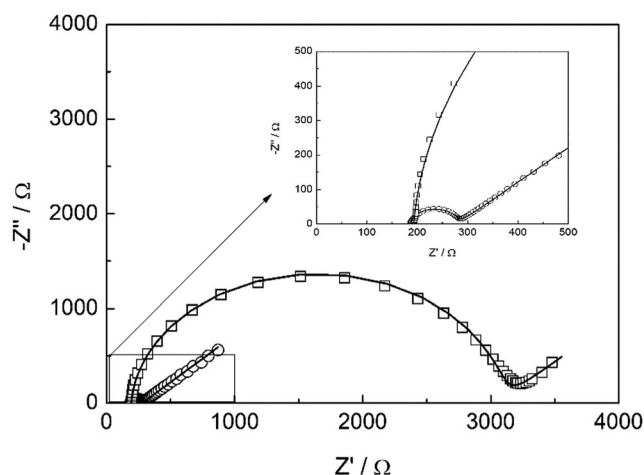


Fig. 4 EIS Nyquist diagram obtained in 5.0 mM K₃Fe(CN)₆/K₄Fe(CN)₆ solution containing 0.10 M KCl for: (○) SPE and (□) poly(4-APA)/SPE. The solid lines represent the experimental data simulation for an equivalent circuit. Amplitude = 10 mV. Frequency range: 10⁵ to 10⁻² Hz. $E_{ap} = OCP$

Warburg impedance, which is related to the diffusion processes that occur in the system, also decreased. This is due to the fact that the deposited film displays anionic characteristics, as do the species present in the analysis solution, which leads to impediment of these negative species in approaching the electrode/solution interface, making it difficult for them to diffuse.

3.4 rNS1 antigen immobilization

In the rNS1 immobilization step, the antigen concentration was varied, with the best results being obtained with 1.0 ng/mL, considering the EIS profile obtained and the adjustment to the proposed equivalent circuit for simulation of the experimental data. The poly(4-APA)/SPE impedance spectrum was compared with that of the rNS1/poly(4-APA)/SPE, and the results are shown in Fig. 5.

It can be observed that rNS1 was immobilized onto the poly(4-APA)/SPE, as shown by the 86% increase in the R_{ct} value from 2876 to 5356 Ω, indicating the formation/adsorption of a new layer on the electrode surface. The high

Table 1 Parameters obtained from the EIS simulation results for SPE and poly(4-APA)/SPE

Parameters	SPE	poly(4-APA)/SPE
$R_s / \Omega \text{ cm}^2$	187	193
$R_{ct} / \Omega \text{ cm}^2$	92.5	2876
$Q_{dl} / \mu\Omega^{-1} \text{ s}^n \text{ cm}^{-2}$	1.75	1.57
n_{dl}	0.94	0.96
$W / \text{m}\Omega^{-1} \text{ s}^{0.5} \text{ cm}^{-2}$	3.18	2.46
$\chi^2 \times 10^{-3}$	3.44	6.06

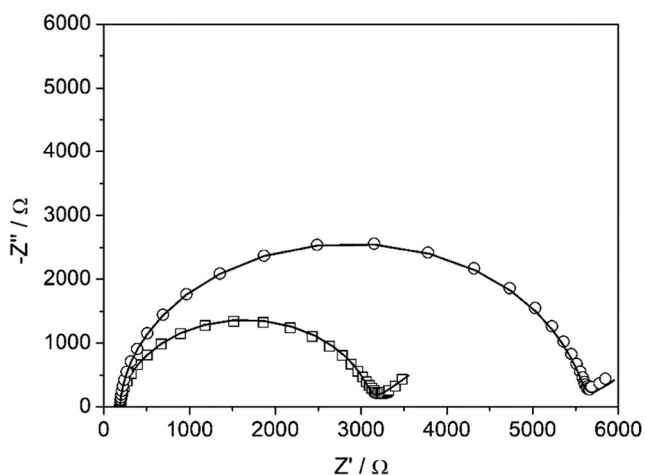


Fig. 5 EIS Nyquist diagram obtained in 5.0 mM $K_3Fe(CN)_6/K_4Fe(CN)_6$ solution containing 0.10 M KCl for: (□) poly(4-APA)/SPE and (○) rNS1/poly(4-APA)/SPE. [rNS1] = 1.0 ng/mL. Amplitude = 10 mV. Frequency range: 10^5 to 10^{-2} Hz. E_{ap} = OCP

resistance found for the rNS1/poly(4-APA)/SPE was due to the adsorption of an antigen layer on the electrode surface modified with the poly(4-APA) film, which presented characteristics that block the electronic transfer that occurs at the electrode/solution interface, which was confirmed by the increase in the R_{ct} value. This is due to the fact that at pH 7.40, NS1 is negatively charged (Bletchly 2002). Since the $[(FeCN)_6]^{3-/4-}$ probe is also anionic, repulsion may occur between the negative species present in the solution and those immobilized on the electrode surface, hindering the probe redox process.

The immunoreaction time was also studied, and it was observed that the best immunoreaction time was 20 min. At shorter times, we could not see a significant difference

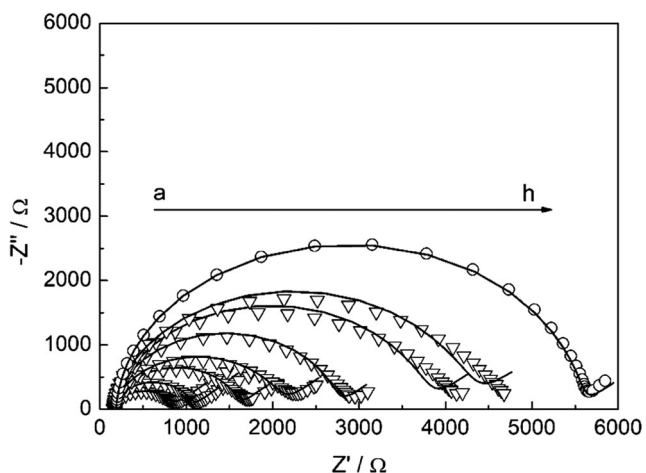


Fig. 6 EIS Nyquist diagram obtained in 5.0 mM $K_3Fe(CN)_6/K_4Fe(CN)_6$ solution containing 0.10 M KCl for: (○) rNS1/poly(4-APA)/SPE at the following positive serum dilutions (V): (a) 1:20; (b) 1:40; (c) 1:80; (d) 1:160; (e) 1:320; (f) 1:640; and (g) 1:1280. The solid lines represent the experimental data simulation for an equivalent circuit. Amplitude = 10 mV. Frequency range: 10^5 to 10^{-2} Hz. [rNS1] = 1.0 ng/mL. E_{ap} = OCP

between the R_{ct} values, and at longer times, stability of R_{ct} values was observed; therefore, the immunoreaction time was chosen as 20 min.

Clinical human serum samples were used at different dilutions to verify the working range and the sensitivity of the proposed methodology. The effect observed in Fig. 6 can be explained by considering the isoelectric point (pI) of the NS1 protein, which is 5.70 (Bletchly 2002). At pH 7.40, NS1 is negatively charged. Since the $[(FeCN)_6]^{3-/4-}$ probe is anionic, there is some resistance to electronic transfer at the electrode/solution interface. In this way, the reduction and/or oxidation of electroactive species on the electrode surface becomes more difficult.

IgG and IgM antibodies presented pI values in the 6.6–7.2 and 5.5–7.4 range, respectively (Agrisera 2018). At pH 7.40, which was used in the present study, IgG and IgM are electrically neutral. Negatively charged rNS1 therefore induces charges on anti-NS1 antibodies; thus, Ag – Ab immunocomplex formation occurs. As a greater number of Ag – Ab complexes are formed, the electron transfer resistance decreases, facilitating electron exchange between the redox probe electroactive species and the modified electrode. Therefore, at higher concentrations (higher serum sample dilution factor), there is not a large amount of anti-NS1 antibodies to form Ag – Ab complexes; and thus, the observed R_{ct} is higher and closer to the R_{ct} value of the rNS1/poly(4-APA)/SPE as compared with higher concentrations (lower serum sample dilution factor), at which there is a larger amount of anti-NS1 antibodies, and consequently, a greater number of Ag – Ab complexes is formed, presenting a lower R_{ct} value.

Evaluation of negative serum samples was carried out to verify the presence of non-specific interactions between the biomolecules present in the serum and the rNS1 protein, as well as potential interferents. Table 2 shows the R_{ct} values obtained with the negative serum sample dilutions as compared with those obtained with the positive serum sample dilutions. R_{ct} values decreased for the negative serum samples at lower dilutions; however, these values were closer to the R_{ct}

Table 2 Comparison between the R_{ct} values for the immunosensor response against serum samples positive and negative for dengue

Dilution factor	R_{ct} (Ω) Positive serum	R_{ct} (Ω) Negative serum	Difference (Ω)
1:20	642	2463	1821
1:40	878	2799	1921
1:80	1408	2964	1556
1:160	1910	3274	1364
1:320	2558	3437	879
1:640	3586	4065	479
1:1280	4091	4585	494
rNS1	5360 Ω		

of the rNS1/poly(4-APA)/SPE (5360 Ω) as compared with the positive serum.

From Table 2, it can be observed that both positive and negative serum samples had an analytical response; however, the signal differentiation obtained with the positive serum samples was significantly higher than that obtained with the negative samples as compared with the rNS1 signal.

It can be observed that the negative serum presented high R_{ct} values, closer to that of rNS1, indicating the occurrence of nonspecific interactions between immobilized rNS1 and DENV antibodies. Comparison of the values in Table 2 shows that even for the highest dilution (1:1280) there was a difference of approximately 10% between R_{ct} values for the negative and positive serum samples. At a 1:20 dilution, a signal decrease of approximately 88% for positive serum and 54% for negative serum was noted as compared with the R_{ct} for the rNS1/poly(4-APA)/SPE.

The differentiation between positive and negative serum samples was more evident at lower dilutions. At a 1:20 dilution, the difference between responses was approximately 4-fold ($\sim 280\%$); however, with increasing dilutions, the response between the two sera became smaller, showing in this case that it is not possible to distinguish and monitor the disease in very dilute serum samples. Moreover, with increasing dilutions, the response also approached that obtained for rNS1, indicating that the contribution of the Ag – Ab interaction slightly interferes with the signal response, which may be directly related to the amount of material present in the sample and the low analytical signal observed.

For serum dilutions up to 1:160, it was possible to safely distinguish between positive and negative diagnoses of dengue in human serum samples using the proposed immunosensor, with a differentiation of approximately 71%. Table 3 shows the studies present in the literature relating to dengue diagnosis. It can be observed that in practically all cases, the operating principle is based on the detection of

NS1, showing low limits of detection and a considerable working range.

In our work proposal, it was not possible to predict the limit of detection (LOD) for the system, since the analysis is performed by recognizing anti-rNS1 antibodies present in human serum samples. Thus, since serum samples were obtained from patients diagnosed with dengue, and considering that the amount of antibodies may vary from individual to individual, the dosage of these antibodies was not performed, and because of this, their concentration was not considered; therefore, only serum dilution studies were carried out. The present study aimed to develop a qualitative system for dengue diagnosis that is easy to use and can confirm or reject diagnosis of the disease, without the need for antibody quantitation.

3.5 Importance of poly(4-APA) film in rNS1 immobilization

Figure 7a shows Nyquist plots for the immobilization of rNS1 on the SPE, and the interaction of positive serum samples with the immunosensor. A small increase in R_{ct} values was observed when comparing the SPE with the rNS1/SPE and with positive serum immobilized directly on the electrode surface ($Ab^+/rNS1/SPE$), without the presence of the poly-4(APA) film, which may be related to poor adsorption of the biological component on the transducer surface.

The electronic transfer resistance value increased by approximately 7% (from 156 to 167 Ω , with $\Delta R_{ct} = 11 \Omega$) from the rNS1/SPE to the $Ab^+/rNS1/SPE$, evidencing that the system was not able to recognize the analyte in the sample. Comparison of this result with those shown in Fig. 6 (also see Fig. 7b) shows that the presence of the polymer film deposited on the electrode surface directly influenced the analytical signal measured, resulting in a higher R_{ct} value. This shows the importance of the functionalized platform in the

Table 3 Studies reported in the literature relating to the diagnosis of dengue, type of transducer, analyte, limit of detection, and working range

Transducer	Analyte	Limit of detection	Working range	Reference
Electrochemical	NS1	12 ng/mL	40–2000 ng/mL	(Dias et al. 2013)
	Protein E	0.94 ng/mL	1–175 ng/mL	(Cavalcanti et al. 2012)
	NS1	15 ng/mL	40–600 ng/mL	(Silva et al. 2014)
	NS1	30 ng/mL	10–1000 ng/mL	(Cecchetto et al. 2015)
	NS1	0.5 ng/mL	1–25 ng/mL	(Sinawang et al. n.d.)
Piezelectrical	NS1	740 ng/mL	–	(Wu et al. 2005)
	NS1	–	0.1–10 $\mu\text{g/mL}$	(Tai et al. 2006)
Optical	IgM	12 pg/mm^2	–	(Wong et al. 2014)
	IgM	1:10 ⁶	–	(Atias et al. 2009)
	RNA	10 pmol/L	–	(Kwakye and Baemner 2003)
	RNA	0.125 nM	–	(Zaytseva et al. 2005)

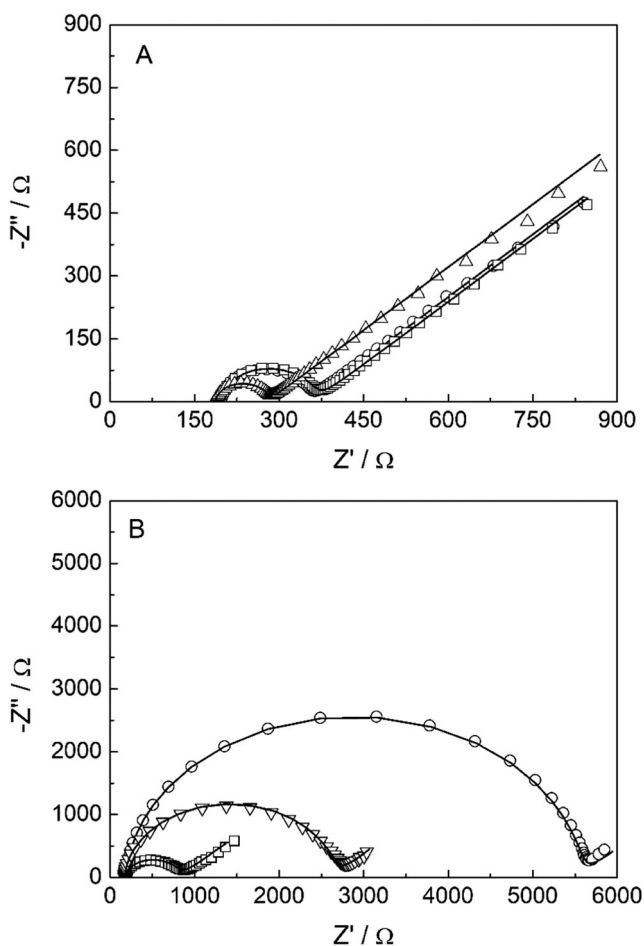


Fig. 7 EIS Nyquist diagram obtained in 5.0 mM $K_3Fe(CN)_6/K_4Fe(CN)_6$ solution containing 0.10 M KCl for: (a) (Δ) SPE; (\circ) rNS1/SPE and (\square) Ab^+ /rNS1/SPE and (b) (\circ) rNS1/poly-4(APA)/SPE; (\square) Ab^+ /rNS1/poly-4(APA)/SPE (∇) Ac^- /rNS1/poly-4(APA)/SPE. The solid lines represent the experimental data simulation for an equivalent circuit. Amplitude = 10 mV. Frequency range: 10^5 to 10^{-2} Hz. Dilution serum: 1:160. [rNS1] = 1.0 ng/mL. E_{ap} = OCP

biomolecule immobilization step, which generates a larger analytical signal.

From Fig. 7b, a significant difference can be observed between the charge transfer resistance of the rNS1/poly(4-APA)/SPE and Ab^+ /rNS1/poly-4(APA)/SPE, showing good sensitivity of the proposed system. For the negative serum, a higher R_{ct} value can be observed as compared with that of the positive serum, which is due to interferants present in the sample matrix that bind nonspecifically to the antigen.

In comparison with the bare immunosensor signal (rNS1), we can say that there was a decrease of 88 and 54% with the positive and negative samples, respectively. In addition, a 74% difference between the positive and negative signals shows high sensitivity of the proposed system.

These results are promising and show the ability of the immunosensor to recognize patients positive for dengue. Moreover, the analyzes were performed without any pretreatment of the samples, and the diagnosis was performed in the

absence of intensive labor and laboratories with specialized equipment.

It was also tested the leaching of the rNS1 by repeating EIS 10 times consecutively both for non-modified SPE and the poly-4AFA/rSPE to verified significant changes on R_{ct} values. It was found an R_{ct} variation of 5.2% for the poly-4AFA/rNS1 and 57.5% for the non-modified SPE. It shows the importance of the polymer film on the immobilization step. The rNS1 and the poly-4AFA keep strongly attached, which is extremely important to the immunoreaction between antigen and Dengue antibodies.

4 Conclusion

The electrogeneration and characterization of the poly(4-APA) film was carried by CV and EIS, and morphological aspects were studied by SEM with which it was possible to verify the presence of the film deposited on the surface of the electrode, via comparison of that prior to and following electropolymerization. The use of this platform was shown to be very promising in the development of an immunosensor for the diagnosis of dengue. It was possible to apply the biosensor to clinical samples from patients infected with dengue virus, and a comparison was made with serum from uninfected patients. This device showed to be very stable, presenting a variation on R_{ct} values of 5.2% after 10 consecutive EIS measurement. It was also observed that for dilutions up to 1:160, it is possible to distinguish between positive and negative serum, with an approximate 71% difference between infected and healthy patients. This difference also suggests high sensitivity of the developed device.

Acknowledgements The authors are grateful for financial support from Conselho Nacional de Desenvolvimento Científico e Tecnológico (CNPq) (Process: 458996/2014-9). The authors wish to thank the LMMMA, sponsored by FAPEMIG (CEX-112-10) and SECTES/MG, for their support. This work is a collaborative research project with the members of the Rede Mineira de Química (RQ-MG), supported by FAPEMIG (Project: CEX - RED-00010-14).

References

- B. Adhikari, S. Majumdar, Polymers in sensor applications. *Prog. Polym. Sci.* **29**, 699–766 (2004). <https://doi.org/10.1016/j.progpolymsci.2004.03.002>
- Agrisera (2018) Molecular weight and isoelectric point of various animal immunoglobulins. 2018 [Cited 2018 07/03/2018]; Available from: <http://www.agrisera.com/en/info/molecular-weight-and-isoelectric-point-of-various-immunoglobulins.html>
- D. Atias, Y. Liebes, V. Chalifa-Caspi, L. Bremand, L. Lobel, R.S. Marks, P. Dussart, Chemiluminescent optical fiber immunosensor for the detection of IgM antibody to dengue virus in humans. *Sensors Actuators B Chem* **140**, 206–215 (2009). <https://doi.org/10.1016/j.snb.2009.03.044>

- Bletchly C (2002) Antigenic and structural analysis of the NS1 glycoprotein of dengue virus. PhD Thesis, University of Queensland
- I.T. Cavalcanti, B.V. Silva, N.G. Peres, P. Moura, M.D. Sotomayor, M.I. Guedes, R.F. Dutra, A disposable chitosan-modified carbon fiber electrode for dengue virus envelope protein detection. *Talanta* **91**, 41–46 (2012). <https://doi.org/10.1016/j.talanta.2012.01.002>
- J. Cecchetto, F.C. Carvalho, A. Santos, F.C.B. Fernandes, P.R. Bueno, An impedimetric biosensor to test neat serum for dengue diagnosis. *Sensors Actuators B Chem* **213**, 150–154 (2015). <https://doi.org/10.1016/j.snb.2015.02.068>
- A.C. Dias, S.L. Gomes-Filho, M.M. Silva, R.F. Dutra, A sensor tip based on carbon nanotube-ink printed electrode for the dengue virus NS1 protein. *Biosens. Bioelectron.* **44**, 216–221 (2013). <https://doi.org/10.1016/j.bios.2012.12.033>
- A.K. Falconar, P.R. Young, Production of dimer-specific and dengue virus group cross-reactive mouse monoclonal antibodies to the dengue 2 virus non-structural glycoprotein NS1. *J. Gen. Virol* **72**, 961–965 (1991). <https://doi.org/10.1099/0022-1317-72-4-961>
- M. Flamand, F. Megret, M. Mathieu, J. Lepault, F.A. Rey, V. Deubel, Dengue virus type 1 nonstructural glycoprotein NS1 is secreted from mammalian cells as a soluble hexamer in a glycosylation-dependent fashion. *J. Gen. Virol.* **73**, 6104–6110 (1999)
- E.A. Henchal, L.S. Henchal, B.K. Thaisomboonsuk, Topological mapping of unique epitopes on the dengue-2 virus NS1 protein using monoclonal antibodies. *J. Gen. Virol.* **68**, 845–851 (1987). <https://doi.org/10.1099/0022-1317-68-3-845>
- E.A. Hunsperger, S. Yoksan, P. Buchy, V.C. Nguyen, S.D. Sekaran, D.A. Enria, J.L. Pelegrino, S. Vázquez, H. Artsob, M. Drebot, D.J. Gubler, S.B. Halstead, M.G. Guzmán, H.S. Margolis, C.M. Nathanson, N.R. Rizzo Lic, K.E. Bessoff, S. Kliks, R.W. Peeling, Evaluation of commercially available anti-dengue virus immunoglobulin M tests. *Emerg. Infect. Dis.* **15**, 436–440 (2009). <https://doi.org/10.3201/eid1503.080923>
- G.C. Júnior, A.P.S. Silva, L.S. Guinesi, Synthesis, characterization and electropolymerization of a new polypyrrole iron (II) Schiff-base complex. *Southeast Asian J. Trop. Med. Public Health* **23**, 1953–1960 (2004). <https://doi.org/10.1016/j.poly.2004.04.029>
- F.M. Kassim, M.N. Izati, T.A. TgRogayah, Y.M. Apanidi, Z. Saat, Use of dengue NS1 antigen for early diagnosis of dengue virus infection. *Southeast Asian J Trop Med Public Health* **42**, 562–569 (2011)
- S. Kwakye, A. Baeumner, A microfluidic biosensor based on nucleic acid sequence recognition. *Anal. Bioanal. Chem.* **376**, 1062–1068 (2003). <https://doi.org/10.1007/s00216-003-2063-2>
- I.M. Mackay, Real-time PCR in the microbiology laboratory. *Clin. Microbiol. Infect* **10**, 190–212 (2004). <https://doi.org/10.1111/j.1198-743X.2004.00722.x>
- D.T. McQuade, A.E. Pullen, T.M. Swager, Conjugated polymer-based chemical sensors. *Chem. Rev.* **100**, 2537–2574 (2000). <https://doi.org/10.1021/cr9801014>
- M.M. Silva, A.C. Dias, M.T. Cordeiro, E. Marques Jr., M.O. Goulart, R.F. Dutra, A thiophene-modified screen printed electrode for detection of dengue virus NS1 protein. *Talanta* **128**, 505–510 (2014). <https://doi.org/10.1016/j.talanta.2014.06.009>
- C.P. Simmons, J.J. Farrar, vV. Nguyen, B. Wills, Dengue. *N. Engl. J. Med.* **366**, 1423–1432 (2012). <https://doi.org/10.1056/NEJMra1110265>
- P.D. Sinawang, V. Rai, R.E. Ionescu, R.S. Marks, Electrochemical lateral flow immunosensor for detection and quantification of dengue NS1 protein. *Biosens. Bioelectron.* **77**, 400–408 (n.d.). <https://doi.org/10.1016/j.bios.2015.09.048>
- V. Somerset, J. Leanera, R. Mason, E. Iwuoha, A. Morrin, Development and application of a poly(2,2'-dithiodianiline) (PDTDA)-coated screen-printed carbon electrode in inorganic mercury determination. *Electrochim. Acta* **55**, 4240–4246 (2010). <https://doi.org/10.1016/j.electacta.2009.01.029>
- D.F. Tai, C.Y. Lin, T.Z. Wu, J.H. Huang, P.Y. Shu, Artificial receptors in serologic tests for the early diagnosis of dengue virus infection. *Clin. Chem.* **52**, 1486–1491 (2006). <https://doi.org/10.1373/clinchem.2005.064501>
- K.F. Tang, E.E. Ooi, Diagnosis of dengue: An update. *Expert Rev. Anti-Infect. Ther.* **10**, 895–907 (2012). <https://doi.org/10.1586/eri.12.76>
- J. Wang, Portable electrochemical systems. *Trends Anal. Chem* **21**, 226–232 (2002). [https://doi.org/10.1016/S0165-9936\(02\)00402-8](https://doi.org/10.1016/S0165-9936(02)00402-8)
- J. Wang, Nanomaterial-based electrochemical biosensors. *Analyst* **130**, 421–426 (2005)
- S.M. Wang, S.D. Sekaran, Evaluation of a commercial SD dengue virus NS1 antigen capture enzyme-linked immunosorbent assay kit for early diagnosis of dengue virus infection. *J. Clin. Microbiol.* **48**, 2793–2797 (2010). <https://doi.org/10.1128/JCM.02142-09>
- W.R. Wong, O. Krupin, S.D. Sekaran, F.R. Mahamd Adikan, P. Berini, Serological diagnosis of dengue infection in blood plasma using long-range surface plasmon waveguides. *Anal. Chem.* **86**, 1735–1743 (2014). <https://doi.org/10.1021/ac403539k>
- World Health Organization (2012) Global strategy for dengue prevention and control 2012-2020. WHO report <http://www.who.int/denguecontrol/9789241504034/en>. Accessed 30 March 2018
- World Health Organization (2017) Dengue and severe dengue. WHO <http://www.who.int/mediacentre/factsheets/fs117/en>. Accessed 30 March 2018
- T.Z. Wu, C.C. Su, L.K. Chen, H.H. Yang, D.F. Tai, K.C. Peng, Piezoelectric immunochip for the detection of dengue fever in viremia phase. *Biosens. Bioelectron.* **21**, 689–695 (2005). <https://doi.org/10.1016/j.bios.2004.12.019>
- N.V. Zaytseva, R.A. Montagna, A.J. Baeumner, Microfluidic biosensor for the serotype-specific detection of dengue virus RNA. *Anal. Chem.* **77**, 7520–7527 (2005). <https://doi.org/10.1021/ac0509206>